Revision 1
Sulfate bearing deposits at Dalangtan playa and its implication for the formation and preservation of Martian salts

W. G. Kong[1*], M. P. Zheng[1], F. J. Kong[1], and W. X. Chen[1]
MLR Key Laboratory of Saline Lake Resources and Environments, Institute of Mineral Resources, CAGS, Beijing 100037, China

Abstract

The sulfate bearing strata on Mars must have recorded rich information of its aqueous history. However, the hydrated sulfates observed in the surface thin layer by remote sensing, especially widespread kieserite, are likely weathering products other than pristine deposits. Here we report the results from the mineralogical investigations and environmental monitoring on the sulfate bearing Dalangtan Playa (an analogue site with Mars-like environmental conditions in northern Tibetan Plateau) to examine the depositional and secondary processes of hydrated sulfates. The regional deposition characters of DLT Playa were described based on our mineralogical results. Widespread kieserite was identified *in situ* by portable laser Raman spectrometer on the weathered surface of the Mg-sulfates rich section, which formed from the hexahydrite dehydration after exposed to the ambient conditions in six months covering the summer, and survived in the winter. During summer days, wind and sunlight may have facilitated the dehydration process, leading the formation of kieserite from dehydration. On the basis of the observed kieserite formation, the recorded local environment conditions, as well as previously reported phase diagrams for Mg-sulfates, we suggest that the current diurnal relative humidity-temperature circles at low latitudes of Mars favor the formation of kieserite through secondary processes.

Key words: Mars analogues; Tibetan Plateau; DLT Playa; sulfates deposits ; Martian kieserite

Introduction:

Various minerals closely related to the aqueous history of Mars have been identified or indicated, including clays (e.g. Bishop et al. 2008; Carter et al. 2010; Ehlmann et al. 2009; Glotch et al. 2006; Mustard et al. 2008; Wang et al. 2006a), carbonates (e.g. Boynton et al. 2009; Carter and Poulet, 2012; Ehlmann et al. 2008; Michalski and Niles 2010; Morris et al. 2010), sulfates (e.g. Arvidson et al. 2005; Gendrin et al. 2005; Kounaves et al. 2010; Langevin et al. 2005; Lichtenberg et al. 2010; Murchie et al. 2009; Squyres et al. 2006; Wang et al. 2006b), and chlorides (Glotch et al., 2010; Jensen and Glotch, 2011; Murchie et al. 2009a; Osterloo et al. 2008, 2010; Ruesch et al. 2012; Wray et al. 2009). It is reasonable to get information on the aqueous history of Mars from the detailed study of these minerals.

Abundant calcium sulfates, mostly gypsum occur near the north polar region of Mars (Langevin et al. 2005). Mg-sulfates have the largest quantities and widest distribution at low latitudes of Mars. For example, those discovered by Observatoire pour la Minéralogie, l'Eau, les Glaces et l'Activité (OMEGA) fill most part of Valleys Marineris and nearby lowlands (Gendrin et al. 2005). Stratigraphic relations of sulfates with different hydration degrees (poly- and monohydrated sulfates) were reported on the basis of comprehensive orbital data sets (Mangold et al. 2008), and clarified for the Martian light-tone layered deposits (ILD) at various sites combining the high resolution Compact Reconnaissance Imaging Spectrometer for Mars (CRISM) with the Context Camera (CTX) data sets (e.g. Bishop et al. 2009; Flahaut et al. 2010; Lichtenberg et al. 2010; Milliken et al. 2010; Murchie et al. 2009a, 2009b; Roach et al. 2009, 2010; Wiseman et al. 2010), and kieserite (monohydrated Mg-sulfate) was specified to be widespread at low latitudes (e.g. Arvidson et al. 2005; Bishop et al. 2009; Gendrin et al. 2005; Mangold et al. 2008; Roach et al. 2009).

The hydration states of sulfates are strongly influenced by the relative humidity

(RH) and temperature (T) of ambient environments. Thus the hydrated sulfates on Martian surface might be the products from the weathering of primary deposits under Mars atmosphere. Many studies through laboratory experiments or thermodynamic modeling have been carried out to investigate the stability properties under different RH and T conditions for sulfates (e.g., Chipera and Vaniman 2007; Chou and Seal 2003, 2007; Grevel et al. 2012; Kong et al. 2011; Steiger et al. 2011; Vaniman et al. 2004, 2006b; Wang et al. 2009, 2011; Xu and Parise 2012), as well as for sulfates associated with smectites under Mars-like RH and T conditions (Wilson and Bish, 2012). These studies have provided critical information for discussing how these observed hydrated sulfates originate.

In nature, complex factors might be involved to constrain the occurrence of specific sulfate species, thus studies on terrestrial analogue sites with similar mineralogy and environmental conditions are needed to help linking these fundamental studies with Mars observations.

Terrestrial analogue studies have focused on various aspects and have served critical information for Mars explorations (e.g. Bishop et al. 2001, Marchant and Head 2007) Since 2008, we have started the expedition at saline playas in a hyperarid region on Tibet Plateau, a terrestrial Mars analogue site, to investigate the mineralogy, geology, bio-signatures, and climatic conditions (Kong et al. 2009, 2013a, 2013b; Mayer et al. 2009; Sobron et al. 2009; Wang and Zheng 2009; Zheng et al. 2009). In this report, we focus on the depositional and weathering processes of hydrated sulfates in one of these saline playas (i.e., Dalangtan Playa).

Dalangtan Playa on Tibetan Plateau

Dalangtan (DLT) Playa formed from the drying up of sulfate brine in the centered depression of the DLT secondary basin (38°0′-38°40′N, 91°10′- 92°10′E, Figure 1)

that locates on the north-west of Qaidam Basin, northern margin of the Tibetan Plateau. The Tibetan Plateau (average elevation of about 4500 m) blocks the humid air carried by the Indian monsoon, leading to the hyperarid (Aridity Index (AI) < 0.04) Qaidam Basin (32-35° N, 90-100° E) (Zheng et al. 2009). DLT basin is the depositional center of the western Qaidam Basin and the high elevation (~ 3000 m) of the DLT Playa induces a low mean annual temperature (276-278 K) as well as the large diurnal, seasonal temperature variation (from 303 K to 253 K) (Kong et al. 2013a). The combination of these factors (sulfate rich sediments, cold and dry weather, low pressure, and high UV radiation) makes the DLT Playa one of the best sites to carry out Mars analogue studies.

Samples and methods

Sample collection

In the recent two expeditions to DLT Playa (September 2012, and January 2013), four vertical sections (i.e. DP1, 2, 3, and 4; 2-4 meters depth) have been sampled at locations with different distances to its depositional center (Figure 1). The sections were made during mining activities and have a depth of 2-4 m. All these four sections exhibit obvious interbedded layers (e.g. Figure 2 for DP2), and fresh samples were systematically collected and numbered on the each layer after removing the weathered crust.

In situ Raman analysis at DLT:

During the expeditions, we used a portable Raman spectrometer (iRaman 532, BW Tec, spectral resolution 4cm^{-1}) for *in situ* characterization of the original deposition sequence as well as the weathered surface for the sulfate-bearing sections (Figure 2). For sections DP1, 3, 4, the Raman spectrometer was used to measure the fresh digged surfaces before sampling. For DP2 section, the Raman spectrometer was used to

carefully examine the mineral phases in the weathered materials on the outer surface.

Laboratory mineralogical analysis of collected samples:

Samples were well sealed and stored in a 233 K freezer to prevent unexpected phase change due to dehydration or rehydration after delivered back (about one week for delivery). For mineralogy characterization, each sample was analyzed by X-ray diffraction (XRD), laser Raman spectroscopy and polarizing petrographic microscopy. The samples used for these measurements were carefully chosen, for example, we only use coarse blocky samples that did not show any feature from dehydration or rehydration.

Laboratory laser Raman analysis was conducted using a Renishaw System-2000 spectrometer (514 nm laser and spectral resolution, 1-2 cm^{-1}) for point measurement on all samples. The laser wavelength calibration was made using a Si wafer and resulted in Raman peak position accuracy of 1 cm^{-1} and precision of 0.5 cm^{-1}.

XRD measurements were carried out on an X-ray diffractometer (Y500 by CDRIG Ltd.) with Cu X-ray source, and all the XRD patterns were collected in the 2θ range of 3-80 °, with step size of 0.05 °. The peak positions were calibrated using the Si (111) spacing of a standard Si reference powder. All samples were measured immediately after they were grounded into powder by either an electric grinder or by an agate mortar. The total duration for the preparation and measurement of single sample is less than one hour.

A Zeiss Axio Scope A1 polarized petrographic microscope was used to determine the mineralogy for all samples, and sulfates with different hydration states can be distinguished based on their different optical properties.

Relative humidity and temperature (RH-T) monitoring

A RHT10 data logger with a capacitance sensor by Extech was placed at the

surface of studied areas for more than two years (since 2010) to record the RH-T conditions near the surface. RH-T conditions were measured and recorded simultaneously every per hour, and the recorded data were collected manually for every 3-6 months.

The RH values at subzero temperatures measured by the RHT10 logger were defined by actual H_2O partial pressure in the air over saturated H_2O partial pressure of ice, and these RH values were transformed to actual H_2O partial pressure in the air over saturated H_2O partial pressure of hypothetical supercooled pure water (i.e. RH% defined by the World Meteorological Organization) based on the Goff–Gratch equation (McDonald, 1965). And the RH values at subzero temperatures in this study all follow the definition by the World Meteorological Organization.

Depositional characters

Table 1 shows the chemical formula for the minerals involved in this study. The minerals identified in different layers of four sampled sections are listed in Table 2, and the order of appearance of each mineral indicates the estimated relative abundance (from large to small) in the layers. Epsomite can be easily dehydrated to hexahydrite even by grinding in XRD sample preparing (Wang et al., 2009), and the pristine Mg-sulfate phase in DP2 was determined to be hexahydrite based on the facts that: 1) hexahydrite was found to be the only Mg-sulfate in the analysis of well stored DP2 samples using petrographic microscope; and 2) none of XRD patterns of DP2 samples showed any signal of epsomite.

The uppermost layer (i.e. the weathered crust), rich in aeolian sands, is thicker in DP 3, 4 sections than in DP1 and 2, indicating an earlier dry up time at the edge of the depression, which is consistent with previous studies (e.g. Wang et al. 1993). Mirabilite dominates in the lower layers for DP 3 and DP 4, followed by the halite

dominating layers, while hexahydrite dominates in DP 2, showing an evolution of sulfate brine from the stage for mirabilite precipitation to that for hexahydrite precipitation, which is common on earth for both lacustrine and marine sediments. Halite occurs in almost all the deposited layers, which indicates that the sulfate brines that formed the studied sections are saturated with NaCl.

The Mg-sulfate bearing DP2 is of the greatest interest among four sections for this study, which serves good opportunity to compare with Mg-sulfates on Mars. Five hexahydrite layers have been noticed in this section (Table 2), and carnallite was found to co-occur with hexahydrite in two of these five layers. Although K-Mg-Cl-SO_4 brines had reached a late stage for the co-precipitation of hexahydrite and carnallite, the brines need to be further concentrated to reach the stage for kieserite precipitation (e.g. Braitsch 1971; Harvie and Weare, 1980).

Apparent mineralogical differences have been found among the interbedded layers for section DP2 (Figure 2). Dark colored layers are rich in clays, which indicate increased supply of fresh waters under relatively wet climates. Whitish layers, dominated by hexahydrite and halite, have less or even no clays, thus would have formed under relatively dry climates with little or no fresh water supply (Zheng et al. 1997).

Kieserite formation at DLT Playa

The DP2 section was created in April 2012 by local mining activities and has been exposed to the ambient atmosphere for about 6 months before our first expedition (Sept. 2012). Kieserite was identified by *in situ* Raman measurements (e.g. the kieserite spectra in Figure 3C) from the whitish materials covering the surface of all five hexahydrite bearing layers in DP2 (Figure 2) for the two expeditions. The kieserite must have formed from the weathering of the hexahydrite layers during the

six months before the first expedition in Sept. 2012, and survived in the winter until the second expedition in Jan. 2013.

Some *in situ* Raman spectra acquired on the pseudomorphic whitish materials (Figure 3B) that came from the hexahydrite dehydration do not show any spectral feature, and further observations under petrographic microscope for these whitish materials suggested the existence of amorphous Mg-sulfates. The Raman spectra of amorphous Mg-sulfates obtained in the laboratory laser Raman measurements do show a broadened peak at 1030 cm^{-1}, however, this peak did not show up in our spectra due to the low sensitivity of the portable Raman spectrometer. Kieserite was also identified several millimeters deeper in these pseudomorphic materials.

We excavated a horizontal section (at 1.5 meter depth) at DP2, from surface to interior for about 15 centimeters. In situ Raman measurements were made at individual spots on this section. The hydrous Mg-sulfates identified on the horizontal section show a trend of increasing hydration degree from the outermost weathered surface to the fresh interior, and they are kieserite and sanderite, starkeyite, pentahydrite, and finally hexahydrite (Figure 3). This clear trend from monohydrated kieserite to the primary hexahydrite indicates a gradient of RH-T conditions within the subsurface that controlled the dehydration/rehydration processes of Mg-sulfates at DP2 site.

The RH-T stability fields of hydrated Mg-sulfates were substantially studied by different experimental methods at temperatures above 263 K (Chou et al. 2003, 2007; Chipera and Vaniman 2007; Peterson and Wang 2006; Steiger et al. 2011; Wang et al. 2009, 2011), and was extrapolated to as low as 175K through thermodynamic calculation (Figure 4, Steiger et al. 2011). Although their results are consistent with each other in general, difference exists referring to the formation of kieserite through

dehydration processes.

In the experiments by Wang et al. (2009) and Chipera and Vaniman (2007), kieserite can only form from dehydration of epsomite or hexahydrite at temperatures above 323 K, and the dehydration stop at starkeyite under DLT relevant temperatures. Starkeyite is metastable under all RH-T conditions (e.g. Chou et al 2007, Steiger et al. 2011), and the dehydration process for starkeyite to kieserite is extremely slow (Steiger et al. 2011). This should be the reason why the dehydration seems to stop at starkeyite in these two sets of experiments (Wang et al. 2009; Chipera and Vaniman 2007). At DP2, the hexahydrite dehydration product, starkeyite, continued to dehydrate at relatively low temperatures (mean annual T 276-278 K, Kong et al. 2013a), and formed widespread kieserite on the outermost surface. In their experiments, constant RH-T conditions were controlled for the dehydration reaction. At DP2, more factors such as wind and sunlight may have been involved in the dehydration process. Wind and sunlight are effective factors to speed up evaporation, and the strong wind and sunlight at DLT Playa (e.g. > 3 m/s for monthly average wind speed at summer, Kong et al. 2013a) may have facilitated the dehydration of starkeyite by quickly removing the water vapor produced from dehydration and by serving more energy for the dehydration reaction respectively, thus kieserite formed at DLT. In the laboratory experiment by Wang et al. 2009, amorphous Mg-sulfates form in the quick dehydration processes, and it cannot form under DLT relevant RH-T conditions. Thus the occurrence of amorphous Mg-sulfates at DLT playa indicates very quick dehydration processes, which was probably induced by wind and sunlight.

Wang et al. (2011) suggested that kieserite can form from the amorphous Mg-sulfates that firstly formed from dehydration under Mars relevant temperatures. At DP2, the amorphous Mg-sulfates overlay or mix with kieserite (Figure 3), and this

232 occurrence does not support that amorphous Mg-sulfates had formed prior to kieserite.
233 Thus we believe that the kieserite at DLT playa mostly formed directly from the
234 dehydration of hexahydrite, and the starkeyite identified (Figure 3) might be the
235 intermediate product of the hexahydrite-kieserite dehydration process.

236 In the work by Steiger et al. (2011), the epsomite-kieserite transition boundary was
237 obtained by a different experimental technique, which suggests kieserite can form
238 from dehydration under DLT relevant temperatures. Our field observation that
239 kieserite formed from the dehydration of hexahydrite at DLT Playta (mean annual T
240 276-278 K and relative humidity < 30%, Kong et al. 2013) give terrestrial evidence to
241 support their results.

242 ## Implications for the observed Mg-sulfates on Mars

243 Although starkeyite is a metastable phase under all RH-T conditions, the
244 dehydration of starkeyite is extremely slow as observed by many experimental studies,
245 thus starkeyite has been suggested to have the most common occurrence under current
246 diurnal RH-T circles on Martian surface (e.g. Steiger et al. 2011 Wang et al., 2011).
247 However, this does not help much on explaining whether the widespread Martian
248 kieserite came from deposition or from the weathering of higher hydrated Mg-sulfates.
249 Our observations of kieserite formation at DLT playa might be able to give some clues
250 referring to this question.

251 The diurnal surface RH-T conditions of a typical summer and a winter day at the
252 DLT playa are shown in Figure 5, and the diurnal RH-T circles have been plotted in
253 Figure 4 for comparison. A typical summer diurnal RH-T circle locates wholly in the
254 RH-T stability field of kieserite (Figure 4), with a diurnal average T of 294 K, and
255 kieserite have formed from hexahydrite dehydration under such conditions in less
256 than 6 months, neglecting the less kieserite favored spring and autumn conditions.

The typical winter diurnal RH-T circle locates wholly outside the kieserite RH-T stability field (diurnal average T of 257 K, Figure 4), however, the previously formed kieserite survived the winter and was detected all over the weathered surfaces of DP2 in our second expedition in Jan. 2013. These facts support previous observation through laboratory experiments that the kieserite formation from dehydration at higher temperatures in the kieserite RH-T stability field is much easier than rehydrating to other phases at lower temperatures outside kieserite field (e.g. Vaniman and Chipera 2006a). And factors such as wind and sunlight make it feasible to observe the kieserite formation from dehydration at DLT Playa.

As indicated by Figure 4, the diurnal RH-T conditions in the Martian summer at low latitudes covers the RH-T stability fields of three stable Mg-sulfates, i.e. kieserite, epsomite, meridianite. At summer daytime on Martian surface, the RH-T conditions locates in the RH-T stability field of kieserite, and wind (with maximum of 7 m/s, Hess et al., 1977) and sunlight can also facilitate the dehydration process of hydrated Mg-sulfates, leading to the formation of kieserite. Although the maximum temperature (255 K) used in this study for Mars is about 48 K lower than that at DLT Playa (303K), the formation of minor amount of kieserite can be expected. Once kieserite had formed during the summer daytime, it has great chance to survive in the low temperature nighttime due to low rehydration rates at the minimum temperature of 195 K, which is about 58 K lower than the minimum temperature in the winter night at DLT Playa (Figure 4). Although the diurnal RH-T circle discussed here is adapted from a summer day, it would be easier for the summer formed kieserite to survive a much colder winter on Mars than that at DLT Playa (Smith et al. 2006; Spanovich et al. 2006). Thus the current diurnal RH-T circles might favor the formation of kieserite.

Beside, RH deviation from equilibrium can also have influence on the dehydration or rehydration rates. However, to our knowledge, no reliable data are available on how much the influence is. For dehydration, there seems no big difference between the RH derivations from equilibrium in daytime on Mars and that in summer at DLT Playa (Figure 4). For rehydration, the RH derivation from equilibrium seems to be larger in nighttime on Mars than that in winter at DLT Playa. However, the temperature decreases as the RH derivation from equilibrium goes larger, which may lead to stronger influence on decreasing the rehydration rates. Thus we believe temperature variations dominate the dehydration or rehydration rates for Mg-sulfates referring to the kieserite formation under current diurnal RH-T conditions on Mars.

If the surface diurnal RH-T circles at low latitude regions on current Mars truly favor the formation of kieserite through dehydration, why are there polyhydrated Mg-sulfates in the vicinity of kieserite bearing regions on Mars as indicated by OMEGA and CRISM observations (e.g. Bishop et al. 2009; Flahaut et al. 2010; Gendrin et al. 2005; Lichtenberg et al. 2010; Milliken et al. 2010; Roach et al. 2009). As reviewed by Murchie et al. (2009a), the polyhydrated sulfates (including Mg bearing phases) tend to occur at stratigraphically higher parts, while kieserite tends to occur at lower parts. We propose that the temperature difference between the atmosphere hundreds of meters above the surface and the surface (about 10 K difference for the first two hundred meters for the Martian atmosphere, Sorbjan et al. 2009) might be one important factor that causes this observed stratigraphic relation for monohydrated and polyhydrated Mg-sulfates. As shown in Figure 4, the hydrated Mg-sulfates on the stratigraphically higher parts have less chance to experience relative high temperatures, thus has a less possibility for dehydrating to kieserite. However, this observed stratigraphic relation is not strict, even interbedded layers of

307 monohydrated and polyhydrated Mg-sulfates were noticed (Roach et al. 2009), and
308 this can be explained by other factors that influences the Mg-sulfate stability
309 properties, such as various abundance of coexisting smectites, which can buffer local
310 RH and prevent the dehydration of coexisting Mg-sulfates (Wilson and Bish 2012).

311 Our scenario for the kieserite formations suggests that the widespread kieserite
312 may have formed through the weathering of hydrated Mg-sulfates under current Mars
313 conditions, which does not require the observed kieserite to be the direct precipitation
314 product from Mg-S-bearing brines.

315 ## Summary

316 Two expeditions have been carried out on DLT Playa (mean annual T 276-278 K ,
317 RH < 30%) in Sept. 2012 and Jan. 2013. The mineralogy of four sulfate bearing
318 sections (DP 1-4) (2-4 meters depth) in this playa were investigated both in situ and
319 on the collected samples in the laboratory. On the basis of obtained mineralogical
320 results, the evolution of the sulfate brines in this region is discussed. All these four
321 sections contain obvious interbedded layers, and hexahydrite was determined to be the
322 major minerals for five layers in section DP2.

323 Hydrated magnesium sulfates including kieserite, sanderite, starkeyite, and
324 pentahydrite have been observed following a trend of increasing hydration state from
325 the weathered surface to the fresh interior.

326 Widespread kieserite was identified on the weathered surface of five hexahydrite
327 bearing layers in DP2 through *in situ* measurements by a portable laser Raman
328 spectrometer for both expeditions. Based on mineralogical results, it is concluded that
329 kieserite observed at DLT came from the dehydration of hexahydrite, and possibly
330 with intermediate product of starkeyite. On the basis of the occurrence of kieserite and
331 stability properties of Mg-sulfates determined by previous studies, we suggest that

factors such as wind and sunlight may have facilitated the dehydration of Mg-sulfates, leading to the quick formation of kieserite at DLT Playa.

Combining our field observations, the surface RH-T data recorded for the DLT Playa, and the RH-T phase diagram of Mg-sulfates determined by previous studies, a scenario is proposed for the formation of widespread Martian kieserite. Our scenario states that the current Mars surface diurnal RH-T circles at low latitudes favor the formation of kieserite through dehydration. The temperature difference between the atmosphere at hundreds of meters above the surface and the surface might be one important factor that controls the stratigraphic trend for monohydrated and polyhydrated Mg-sulfates observed on Mars. In this scenario, the Martian kieserite does not need to be the deposition product from brines, which might be favored by the atmospheric modeling studies for past Mars.

Acknowledgements: This work was supported by the Basic Research and Operating Fund (K0903), the National Geological survey's project (1212011120178), and the National Science Foundation of China (U0833601). Special thanks to Prof. Melinda Dyar for her help on handling this manuscript. We really appreciate constructive suggestions on the manuscript from Prof. Yiliang Li and one anonymous reviewer.

References

Arvidson, R.E., Poulet, F., Bibring, J.-P., Wolff, M., Gendrin, A., Morris, R.V., Freeman, J.J., Langevin, Y., Mangold, N., and Bellucci, G. (2005) Spectral Reflectance and Morphologic Correlations in Eastern Terra Meridiani, Mars. Science, 307, 1591–1594.

Bishop, J.L., Lougear, A. Newton, J. Doran, P.T., Froeschl, H., Trautwein, A.X., Orner, W.K., and Koeberl C. (2001) Mineralogical and geochemical analyses of Antarctic lake sediments: A study of reflectance and Mossbauer spectroscopy

and C, N, and S isotopes with applications for remote sensing on Mars. Geochimica et Cosmochimica Acta, Vol. 65, No. 17. pp. 2875–2897.

Bishop, J.L., Dobrea, E.Z.N., McKeown, N.K., Parente, M., Ehlmann, B.L., Michalski, J.R., Milliken, R.E., Poulet, F., Swayze, G.A., Mustard, J.F., Murchie, S.L., and Bibring, J.P. (2008) Phyllosilicate diversity and past aqueous activity revealed at Mawrth vallis, Mars. Science, 321, 830–833.

Bishop, J.L., Parente, M. Weitz,C.M., Dobrea, E.Z.N., Roach, LH., Murchie, S.L., McGuire, P.C., McKeown, N.C., Rossi, C.M., Brown, A.J., Calvin, W.M., Milliken, R., and Mustard J.F. (2009), Mineralogy of Juventae Chasma: Sulfates in the light-toned mounds, mafic minerals in the bedrock, and hydrated silica and hydroxylated ferric sulfate on the plateau, Journal of Geophysical Research, 114, E00D09.

Bishop J.L. et al. 2013. Refining Martian carbonate chemistries determined through CRISM analyses of several carbonate-bearing outcrops. Lunar and Planetary Science Conference, XLIV, Abstract 2555.

Braitsch, O. (1971) Salt deposits: their origin and composition. 297 p. Springer-Verlag, Berlin, Heidelberg, New York.

Boynton, W.V., Ming, D.W., Kounaves, S.P, Young, SMM, Arvidson, R.E., Hecht, M.H., Hoffman, J, Niles, P.B., Hamara, D.K., Quinn, R.C., Smith, P.H., Sutter, B., Catling, D.C., and Morris, R.V. (2009) Evidence for Calcium Carbonate at the Mars Phoenix Landing Site. Science 325: 61-64.

Carter J. and Poulet F. (2012) Orbital identification of clays and carbonates in Gusev crater. Icarus. 219. 250–253.

Carter, J. Poulet F., Bibring J.-P., and Murchie, S. (2010) Detection of hydrated silicates in crustal outcrops in the northern plains of Mars. Science, 328,

1682–1686.

Chipera, S.J. and Vaniman, D.T. (2007) Experimental stability of magnesium sulfate hydrates that may be present on Mars. Geochimica et Cosmochimica Acta, 71, 241–250.

Chou, I.M. and Seal R.R. (2003), Determination of epsomite-hexahydrite equilibria by the humidity-buffer technique at 0.1 MPa with implications for phase equilibria in the system MgSO4-H_2O, Astrobiology, 3, 619–629,

Chou, I.M. and Seal R.R. (2007) Magnesium and calcium sulfate stabilities and the water budget of Mars, Journal of Geophysical Research, 112, E11004.

Ehlmann, B.L., Mustard, J.F., Murchie, S.L., Poulet, F., Bishop, J.L., Brown, A.J., Calvin, W.M., Clark, R.N., Des Marais, D.J., Milliken, R.E., Roach, L.H., Roush, T.L., Swayze, G.A., and Wray, J.J. (2008) Orbital Identification of Carbonate-Bearing Rocks on Mars. Science, 322, 1828–1832.

Ehlmann, B.L., Mustard, J.F., Swayze, G.A., Clark, R.N., Bishop, J.L., Poulet, F., Des Marais, D.J., Roach, L.H., Milliken, R.E., Wray, J.J., Barnouin-Jha, O., and Murchie, S.L. (2009) Identification of hydrated silicate minerals on Mars using MRO-CRISM: Geologic context near Nili Fossae and implications for aqueous alteration. Journal of Geophysical Research-Planets, 114, E00D08.

Flahaut, J., Quantin, C., Allemand, P., Thomas, P., and Le Deit L. (2010) Identification, distribution and possible origins of sulfates in Capri Chasma (Mars), inferred from CRISM data, Journal of Geophysical Research, 115, E11007.

Gendrin, A., Mangold, N., Bibring, J.P., Langevin, Y., Gondet, B., Poulet, F., Bonello, G., Quantin, C., Mustard, J., Arvidson, R., and LeMouelic, S. (2005) Sulfates in Martian layered terrains: the OMEGA/Mars Express view. Science, 307,

1587–1591.

Glotch, T.D., Bandfield, J.L., Tornabene, L.L., Jensen, H.B., and Seelos F.P. (2010) Distribution and formation of chlorides and phyllosilicates in Terra Sirenum, Mars. Geophysical Research Letters, 37, L16202.

Grevel, K.D., Majzlan, J., Benisek, A., Dachs, E., Steiger, M. Fortes, A.D., and Marler., B. (2012) Experimentally Determined Standard Thermodynamic Properties of Synthetic $MgSO_4 \cdot 4H_2O$ (Starkeyite) and $MgSO_4 \cdot 3H_2O$: A Revised Internally Consistent Thermodynamic Data Set for Magnesium Sulfate Hydrates. Astrobiology, 12, 1042–1054.

Harvie, C.E. and Weare, J.M. (1980) The prediction of mineral solubilities in natural waters: the Na–K–Mg–Ca–CI–SO_4–H_2O system from zero to high concentration at 25 °C. Geochimica et Cosmochimica Acta, 44, 981–997.

Hess, S.L., Henry, R.M., Leovy, C.B., Ryan, J.A., and Tillman J.E. (1977) Meteorological results from the surface of Mars: Viking 1 and 2, Journal of Geophysical Research, 82, 4559–4574.

Jensen, H.B. and Glotch, T.D. (2011) Investigation of the near infrared spectral character of putative Martian chloride deposits. Journal of Geophysical Research, 116, E00J03.

Kong, F.J., Zheng, M.P., Wang, A., and Ma, N.N. (2009) Endolithic halophiles found in evaporite salts on Tibet Plateau as a potential analog for martian life in saline environment. Lunar and Planetary Science Conference, XL, Abstract 1216.

Kong, F.J., Kong, W.G., Hu B., and Zheng M.P. (2013a) Meteorological Data, Surface Temperature and Moisture Conditions at the Dalantan Mars Analogous Site, in Qinghai Tibet Plateau, China. Lunar and Planetary Science Conference,

433 XLIV, Abstract 1743.
434 Kong, W.G., Zheng, M.P., Kong, F.J., Wang, A., Chen W.X., and Hu B. (2013b)
435 Sedimentary salts at Dalangtan Playa and its implication for the formation
436 and preservation of Martian salts. Lunar and Planetary Science Conference,
437 XLIV, Abstract 1336.
438 Kounaves, S. P., Hecht, M. H., Kapit, J., Quinn, R. C., Catling, D. C., Clark, B. C.,
439 Ming, D. W., Gospodinova, K., Hredzak, P., McElhoney, K. and Shusterman,
440 J. (2010) Soluble sulfate in the martian soil at the Phoenix landing site.
441 Geophysical Research Letters, 37, L09201.
442 Langevin, Y., Poulet, F., Bibring, J.P., and Gondet, B. (2005) Sulfates in the north
443 polar region of Mars detected by OMEGA/Mars Express. Science, 307,
444 1584–1586.
445 Lichtenberg, K.A., Arvidson, R.E., Morris, R.V., Murchie, S.L., Bishop, J.L.,
446 Fernandez Remolar, D., Glotch, T. D., Noe Dobrea, E., Mustard, J.F.,
447 Andrews-Hanna, J., and Roach, L.H. (2010) Stratigraphy of hydrated sulfates
448 in the sedimentary deposits of Aram Chaos, Mars. Journal of Geophysical
449 Research, 115, E00D17.
450 Mangold N., Gendrin, A., Gondet, B., LeMouelic, S., Quantin, C., Ansan, V., Bibring
451 J.P., Langevin, Y., Masson, P., and Neukum, G. (2008) Spectral and
452 geological study of the sulfate-rich region of West Candor Chasma, Mars.
453 Icarus, 194, 519–543.
454 Marchant, D.R. and Head, J.W. (2007) Antarctic Dry Valleys: microclimate zonation,
455 variable geomorphic processes, and implications for assessing climate change
456 on Mars. Icarus 192, 187–222.
457 Mayer, D.P., Arvidson R.E., Wang A., Sobron P., and Zheng M.P. (2009) Mapping

458 minerals at a potential mars analog site on the Tibetan plateau. Lunar and
459 Planetary Science Conference, XL, Abstract 1877.
460 Michalski, J.R. and Niles, P.B. (2010) Deep crustal carbonate rocks exposed by
461 meteor impact on Mars. Nature Geoscience, 3, 751–755.
462 Milliken, R.E., Grotzinger, J.P., and Thomson, B.J. (2010) Paleoclimate of Mars as
463 captured by the stratigraphic record in Gale Crater. Geophysical Research
464 Letters, 37, L04201.
465 Morris, R.V., Ruff, S.W., Gellert, R., Ming, D.W., Arvidson, R.E., Clark, B.C., Golden,
466 D.C., Siebach, K., Klingelhöfer, G., Schröder, C., Fleischer, I., Yen, A.S., and
467 Squyres, S.W. (2010) Identification of Carbonate–Rich Outcrops on Mars by
468 the Spirit Rover. Science, 329, 421–424.
469 Murchie, S.L., Mustard, J.F., Ehlmann, B.L., Milliken, R.E., Bishop, J.L., McKeown,
470 N.K., Noe Dobrea, E.Z., Seelos, F.P., Buczkowski, D.L., Wiseman, S.M.,
471 Arvidson, R.E., Wray, J.J., Swayze, G., Clark, R.N., Des Marais, D.J.,
472 McEwen, A.S., and Bibring, J.P. (2009a) A synthesis of Martian aqueous
473 mineralogy after 1 Mars year of observations from the Mars Reconnaissance
474 Orbiter. Journal of Geophysical Research, 114, E00D06.
475 Murchie, S., Roach, L., Seelos, F., Milliken, R., Mustard, J., Arvidson, R., Wiseman,
476 S., Lichtenberg, K., Andrews-Hanna, J., Bishop, J., Bibring, J.P., Parente, M.,
477 and Morris, R. (2009b) Evidence for the origin of layered deposits in Candor
478 Chasma, Mars, from mineral composition and hydrologic modeling. Journal
479 of Geophysical Research, 114, E00D05.
480 Mustard, J.F., Murchie, S.L., Pelkey, S.M., Ehlmann, B.L., Milliken, R.E., Grant, J.A.,
481 Bibring, J.P., Poulet, F., Bishop, J., Dobrea, E.N., Roach, L., Seelos, F.,
482 Arvidson, R.E., Wiseman, S., Green, R., Hash, C., Humm, D., Malaret, E.,

McGovern, J.A., Seelos, K., Clancy, T., Clark, R., Des Marais, D., Izenberg, N., Knudson, A., Langevin, Y., Martin, T., McGuire, P., Morris, R., Robinson, M., Roush, T., Smith, M., Swayze, G., Taylor, H., Titus, T., and Wolff, M. (2008) Hydrated silicate minerals on mars observed by the Mars reconnaissance orbiter CRISM instrument. Nature, 454, 305–309

Osterloo, M.M., Hamilton, V.E., Bandfield, J.L., Glotch, T.D., Baldridge, A.M., Christensen, P.R., Tornabene, L.L., and Anderson, F.S. (2008) Chloride-Bearing Materials in the Southern Highlands of Mars. Science, 319, 1651–1654.

Osterloo, M.M., Anderson, F.S., Hamilton, V.E., and Hynek, B.M. (2010) Geologic context of proposed chloride-bearing materials on Mars. Journal of Geophysical Research, 115, E10012.

Peterson, R.C. and Wang, R. (2006) Crystal molds on Mars: melting of a possible new mineral species to create Martian chaotic terrain. Geology, 34, 957–960.

Roach, L.H., Mustard, J.F., Murchie, S.L., Bibring, J.P., Forget, F., Lewis, K.W., Aharonson, O., Vincendon, M., and Bishop J.L. (2009) Testing evidence of recent hydration state change in sulfates on Mars, Journal of Geophysical Research, 114, E00D02.

Roach, L.H., Mustard, J.F., Swayze, G., Milliken, R. E., Bishop, J.L., Murchie, S.L., and Lichtenberg, K. 2010. Hydrated mineral stratigraphy of Ius Chasma, Valles Marineris. Icarus 206, 253-268.

Ruesch, O., Poulet, F., Vincendon, M., Bibring, J.P., Carter, J., Erkeling, G., Gondet, B., Hiesinger, H., Ody, A., and Reiss D. (2012) Compositional investigation of the proposed chloride-bearing materials on Mars using near-infrared orbital data from OMEGA/MEx. Journal of Geophysical Research, 117,

E00J13.

Saviäjrvi H. (1995) Mars boundary layer modeling: diurnal moisture cycle and soil properties at the Viking Lander 1 site. Icarus, 117, 120–127.

Smith, M.D., Wolff, M.J., Spanovich, N., Ghosh, A., Banfield, D., Christensen, P.R., Landis, G.A., and Squyres S.W. (2006), One Martian year of atmospheric observations using MER Mini-TES. Journal of Geophysical Research, 111, E12S13.

Sobron P., Freeman J. J., and Wang A. (2009) Field test of the water-wheel IR (WIR) spectrometer on evaporative salt deposits at Tibetan plateau. Lunar and Planetary Science Conference, XL, Abstract 2372.

Sorbjan Z., Wolff, M., and Smith, M.D. (2009) Thermal structure of the atmospheric boundary layer on Mars based on Mini-TES observations. Quarterly Journal of the Royal Meteorological Society, 135, 1776–1787.

Spanovich, N., Smith, M.D., Smith, P.H., Wolff, M.J., Christensen, P.R., and Squyres S.W. (2006), Surface and near-surface atmospheric temperatures for the Mars Exploration Rover landing sites. Icarus, 180, 314–320.

Squyres, S.W., Arvidson, R.E., Bollen, D., Bell, J.F., Brückner, J., Cabrol, N.A., Calvin, W.M., Carr, M. H., Christensen, P.R., Clark, B.C. Crumpler, L., Des Marais, D.J., d'Uston, C., Economou, T., Farmer, J., Farrand, W.H., Folkner, W., Gellert, R., Glotch, T.D., Golombek, M., Gorevan, S., Grant, J.A., Greeley, R., Grotzinger, J., Herkenhoff, K.E., Hviid, S., Johnson, J.R., Klingelhöfer, G., Knoll, A.H., Landis, G., Lemmon, M., Li, R., Madsen, M.B., Malin, M.C., McLennan, S.M., McSween, H.Y., Ming, D.W., Moersch, J., Morris, R.V., Parker, T., Rice, J.W. Jr., Richter, L., Rieder, R., Schroeder, C., Sims, M., Smith, M., Smith, P., Soderblom, L.A., Sullivan, R.J., Tosca, N.J.,

Wänke, H., Wdowiak, T., Wolff, M., and Yen, A. (2006) Overview of the Opportunity Mars Exploration Rover Mission to Meridiani Planum; Eagle Crater to Purgatory Ripple. Journal of Geophysical Research, 111, E12S12.

Steiger, M., Linnow, K., Ehrhardt, D., and Rohde M. (2011) Decomposition reactions of magnesium sulfate hydrates and phase equilibria in the $MgSO_4$–H_2O and Na^+–Mg^{2+}–Cl^-–SO_4^{2-}– H_2O systems with implications for Mars. Geochimica et Cosmochimica Acta, 75, 3600–3626.

Vaniman, D.T., Bish, D.L., Chipera, S.J., Fialips, C.I., Carey, J.W., and Feldman, W.C. (2004) Magnesium sulphate salts and the history of water on Mars. Nature, 431, 663–668.

Vaniman, D.T. and Chipera S.J. (2006) Transformations of Mg and Ca-sulfate hydrates in Mars regolith. American Mineralogist, 91:1628–1642.

Vaniman D. T., Chipera S. J. and Carey J. W. (2006) Hydration experiments and physical observations at 193 K and 243 K for Mg-sulfates relevant to Mars. Lunar and Planetary Science Conference, XXXVII, Abstract 1442.

Wang, A., Korotev, R.L., Jolliff, B.L., Haskin, L.A., Crumpler, L., Farrand, W.H., Herkenhoff, K.E., de Souza, P., Kusack, A.G., Hurowitz, J.A., Tosca, N.J. (2006a) Evidence of phyllosilicates in Wooly Patch, an altered rock encountered at West Spur, Columbia Hills, by the Spirit rover in Gusev crater, Mars. Journal of Geophysical Research-Planets, 111, E02S16.

Wang A., Haskin, L.A., Squyres, S.W., Jolliff, B.L., Crumpler, L., Gellert, R., Schroder, C., Herkenhoff, K., Hurowitz, J., Tosca, N.J., Farrand, W.H., Anderson, R., Knudson, A.T. (2006b) Sulfate deposition in subsurface regolith in Gusev crater, Mars. Journal of Geophysical Research-Planets, 111, E02S17.

558 Wang, A., Freeman J.J., Jolliff B.L., and Chou I.M. (2006c), Sulfates on Mars: A
559 systematic Raman spectroscopic study of hydration states of magnesium
560 sulfates, Geochim. Cosmochim. Acta, 70, 6118–6135.
561 Wang, A., Freeman, J.J., and Jolliff B.L. (2009), Phase transition pathways of the
562 hydrates of magnesium sulfate in the temperature range 50C to 5C:
563 Implication for sulfates on Mars. Journal of Geophysical Research, 114,
564 E04010.
565 Wang, A. and Zheng, M.P. (2009) Evaporative salts from saline lakes on Tibet plateau:
566 an analog for salts on mars, Lunar and Planetary Science Conference, XL,
567 Abstract 1858.
568 Wang, A., Freeman, J.J., Chou, I.M., and Jolliff B.L. (2011) Stability of Mg-sulfates at
569 −10°C and the rates of dehydration/rehydration processes under conditions
570 relevant to Mars. Journal of Geophysical Research, 116, E12006.
571 Wang M.L., Wang, Y.J., Liu C.L., and Chen, Y.Z. (1993) The features and genesis of
572 the Dalangtan salt deposit in the Qaidam basin. Bulletin of the Chinese
573 Academy of Geological Sciences, 26, 97-114.
574 Wilson S.A. and Bish D.L. (2012) Stability of Mg-sulfate minerals in the presence of
575 smectites: Possible mineralogical controls on H_2O cycling and biomarker
576 preservation on Mars. Geochimica et Cosmochimica Acta, 96, 120–133.
577 Wiseman, S.M., Arvidson, R.E., Morris, R.V., Poulet, F., Andrews-Hanna, J.C.,
578 Bishop, J.L., Murchie, S.L., Seelos, F.P., Des Marais, D., and Griffes J.L.
579 (2010) Spectral and stratigraphic mapping of hydrated sulfate and
580 phyllosilicate bearing deposits in northern Sinus Meridiani, Mars. Journal of
581 Geophysical Research, 115, E00D18.
582 Wray, J.J., Murchie, S.L., Squyres, S.W., Seelos F.P., and Tornabene L.L. (2009)

583 Diverse aqueous environments on ancient Mars revealed in the southern
584 highlands. Geology, 37, 1043–1046.
585 Xu, W. and Parise, J. (2012) Temperature and humidity effects on ferric sulfate
586 stability and phase transformation. American Mineralogist, 97, 378–383.
587 Zheng, M.P. (1997) An Introduction to Saline Lakes on the Qinghai-Tibet Plateau.
588 Kluwer Acad., Dordrecht, Netherlands.
589 Zheng, M.P., Wang, A., Kong, F.J., and Ma, N.N. (2009) Saline lakes on
590 Qinghai-Tibet Plateau and salts on Mars. Lunar and Planetary Science
591 Conference, XL, Abstract 1454.

592 ## Captions for Figures and tables

593 Figure 1. Location of Dalangtan (DLT) Playa in the Qaidam Basin on Tibetan Plateau.
594 Samples were systematically collected on four sections (DP 1, 2, 3, 4) with different distances
595 to the depositional center of DLT Playa.
596
597 Figure 2. Photo of DP2 section and *in situ* Raman measurements
598
599 Figure 3. Occurrence of hydrated Mg-sulfates at section DP2. A) Photo of a plane
600 perpendicular to the weathered surface of DP2 section excavated for *in situ* Raman
601 investigation. B) Photo of weathered material from section DP2, whitish pseudomorphic
602 crystals come from hexahydrite dehydration, and darker colored halite crystals persist from
603 weathering. C) *In situ* Raman spectra of Mg-sulfates (assigned based on Wang et al. (2006c)),
604 and the markers on photo A (Ks, kieserite; Sa, sanderite; St, starkeyite; Pt, pentahydrite, and
605 Hx, hexahydrite) show where the spectra were obtained. Epsomite cannot be distinguished *in*
606 *situ* from hexahydrite due to limited spectral accuracy of the portable Raman spectrometer
607 (Wang et al. 2006c), and epsomite was ruled out after the XRD and petrographic microscope
608 analysis on collected samples. D) Major sulfate peaks of Raman spectra in C with peaks
609 indicated.
610

Figure 4. Phase diagram of $MgSO_4$-H_2O system at low temperatures (adapted from Steiger et al. (2011)). Dashed curves are the phase boundaries for $11H_2O$-$7H_2O$, $7H_2O$-$6H_2O$, $7H_2O$-$4H_2O$ and $6H_2O$-$4H_2O$, and the dotted line represents the boundary for $6H_2O$-$1H_2O$ (above 293 K) and the $7H_2O$-$1H_2O$ boundary (below 293 K). Solid loop represents a daily cycle of present-day Mars conditions in summer at the Viking Lander 1 site (Savijärvi 1995). The dashed loop shows the diurnal change of the atmospheric conditions hundreds of meters above the surface inferred by Mini-TES on Spirit rover (Sorbjan et al. 2009). Dotted loops indicate the diurnal change of the surface conditions of DLT Playa for a typical summer and winter day, and the specific date is noted in the figure.

Figure 5. Diurnal surface RH-T conditions of the DLT Playa for a typical summer and winter day (specific dates are marked in the figure).

Table 1. Chemical formulas for salt minerals involved in this study.

Table 2. Minerals identified in each layer from the top surface to the bottom of four sections. The order of appearance for each mineral indicates the estimated relative abundance (from large to small) in the layers.

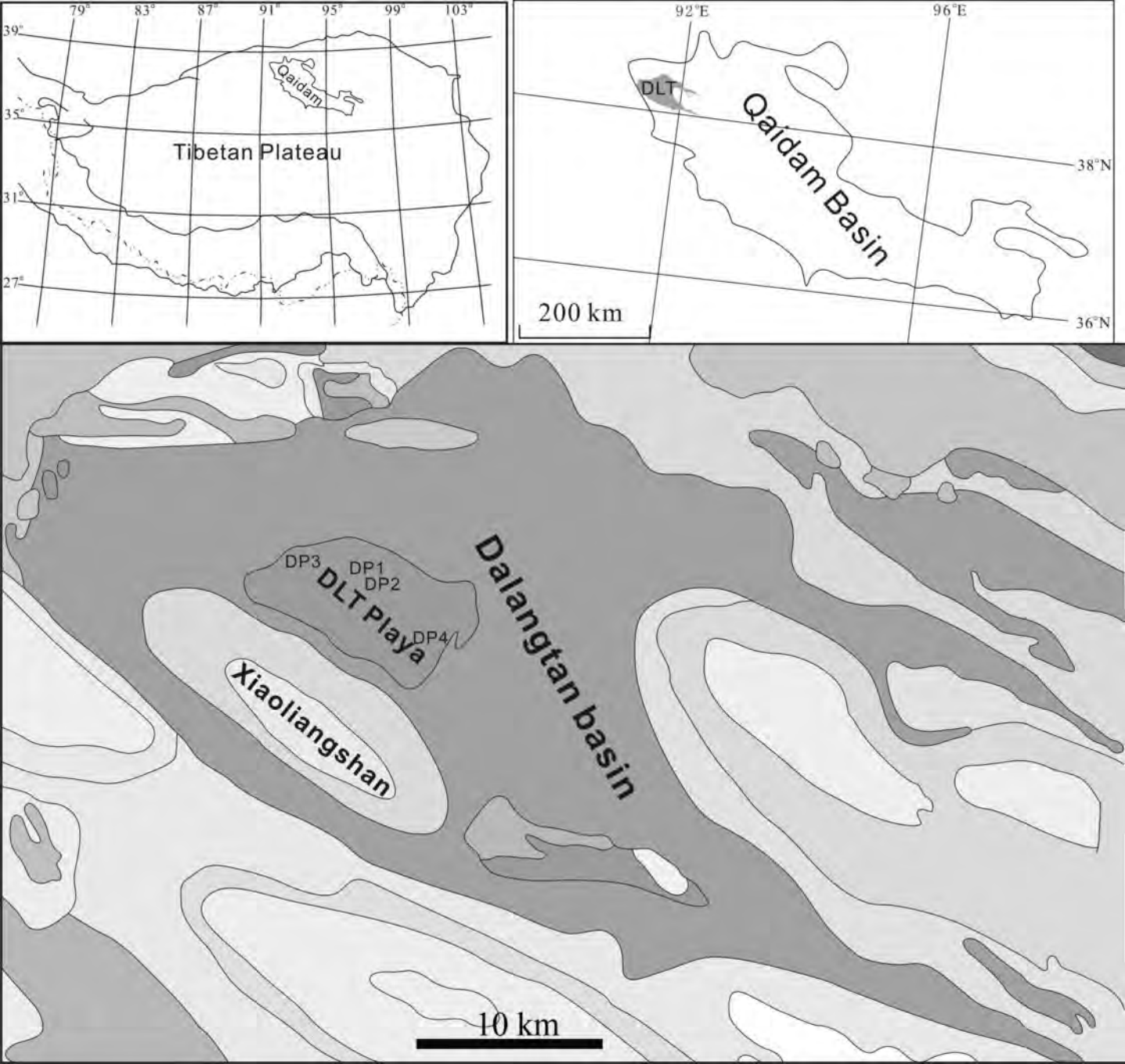
79°
83°
87°
91°
95°
99°
103°
39°
35°
31°
27°
Qaidam
Tibetan Plateau
92°E
96°E
DLT
Qaidam Basin
38°N
36°N
200 km
DP3
DP1
DP2
DLT Playa
DP4
Dalangtan basin
Xiaoliangshan
10 km

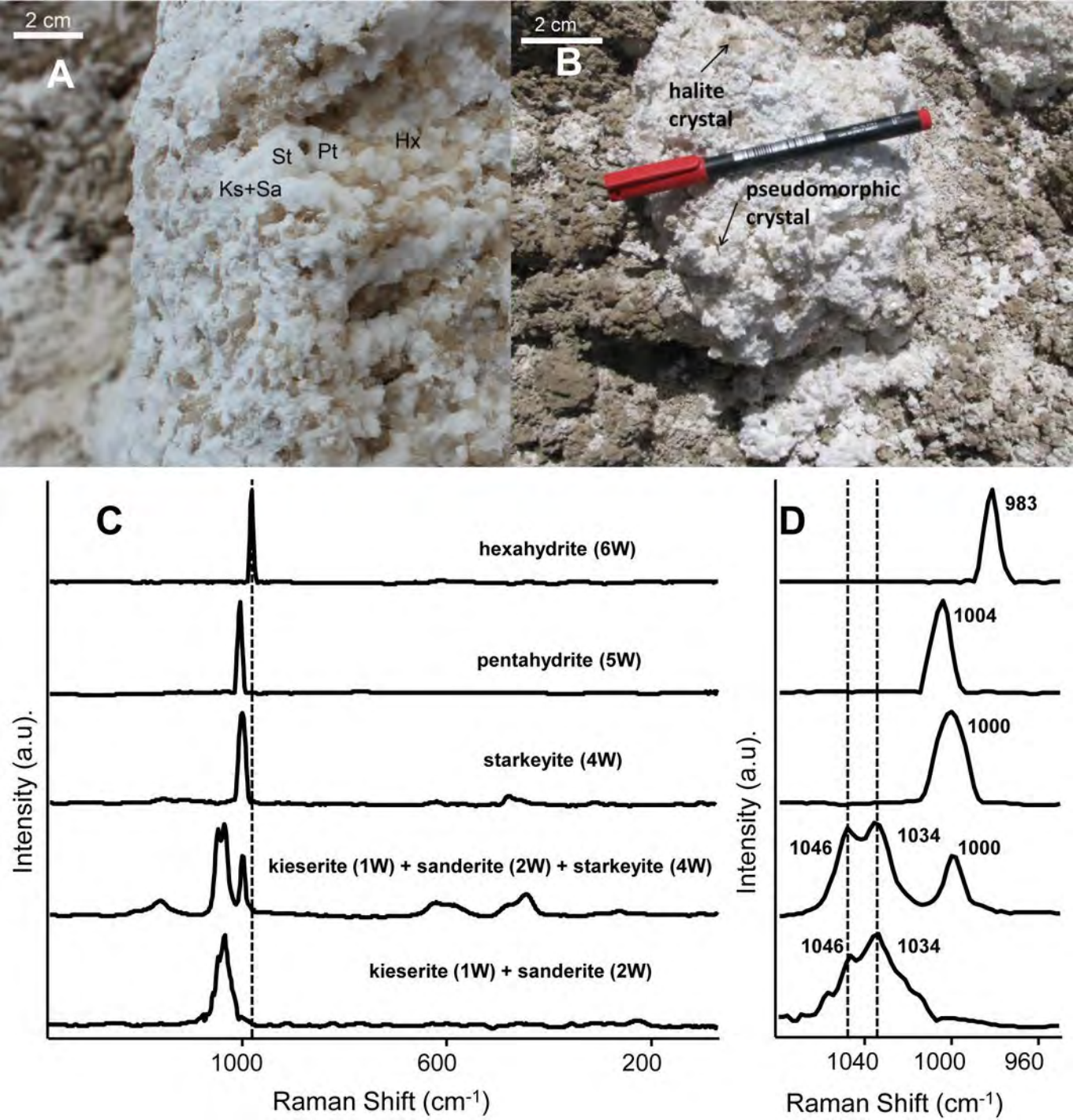
2 cm
A
St
Pt
Hx
Ks+Sa
2 cm
B
halite
crystal
pseudomorphic
crystal
C
hexahydrite (6W)
pentahydrite (5W)
starkeyite (4W)
kieserite (1W) + sanderite (2W) + starkeyite (4W)
kieserite (1W) + sanderite (2W)
Intensity (a.u.).
1000
600
200
Raman Shift (cm-1)
D
983
1004
1000
1046
1034
1000
1046
1034
Intensity (a.u.)
1040
1000
960
Raman Shift (cm-1)

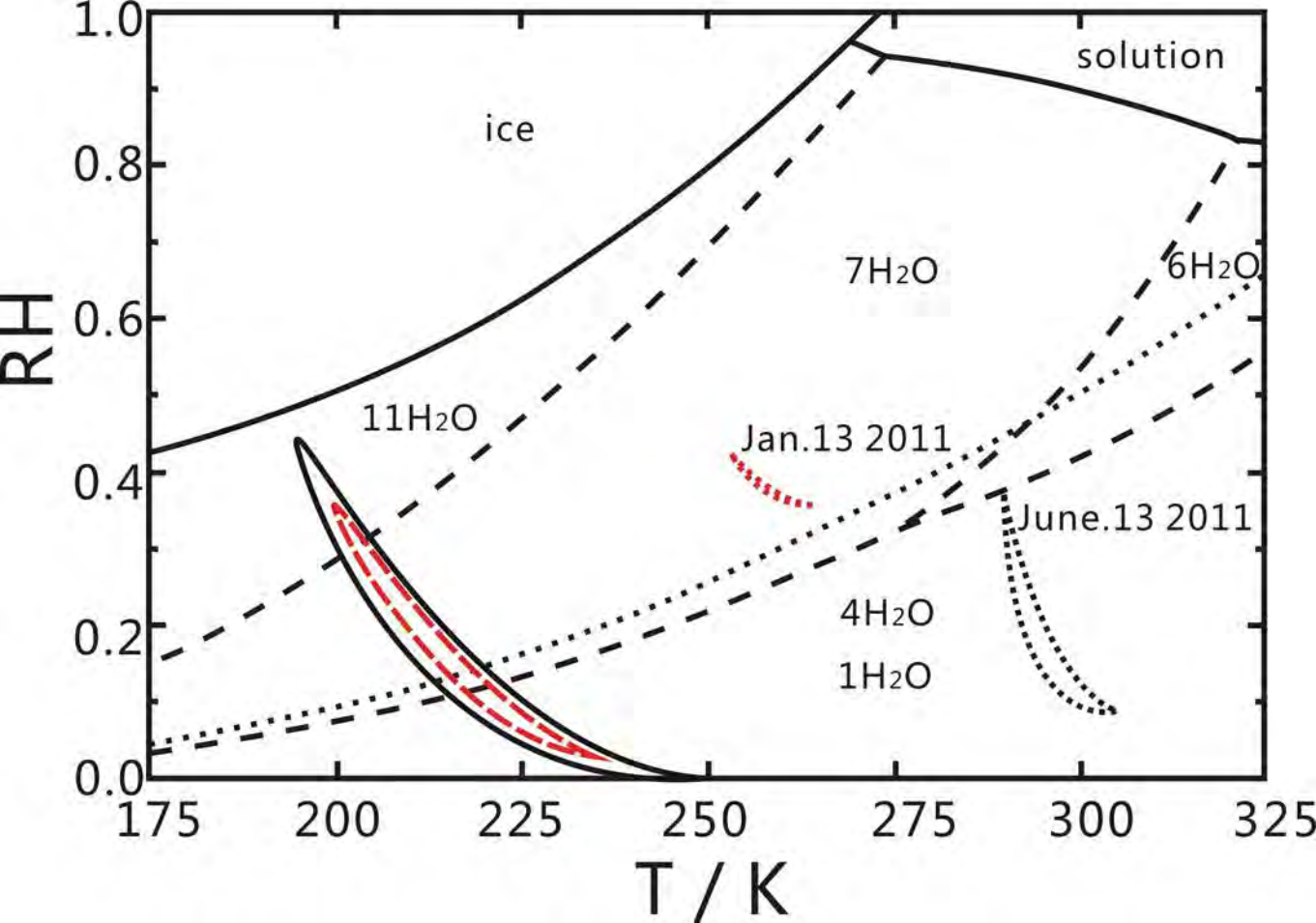
1.0
0.8
0.6
0.4
0.2
0.0
RH
175
200
225
250
275
300
325
T / K
ice
solution
7H2O
6H2O
11H2O
Jan.13 2011
June.13 2011
4H2O
1H2O

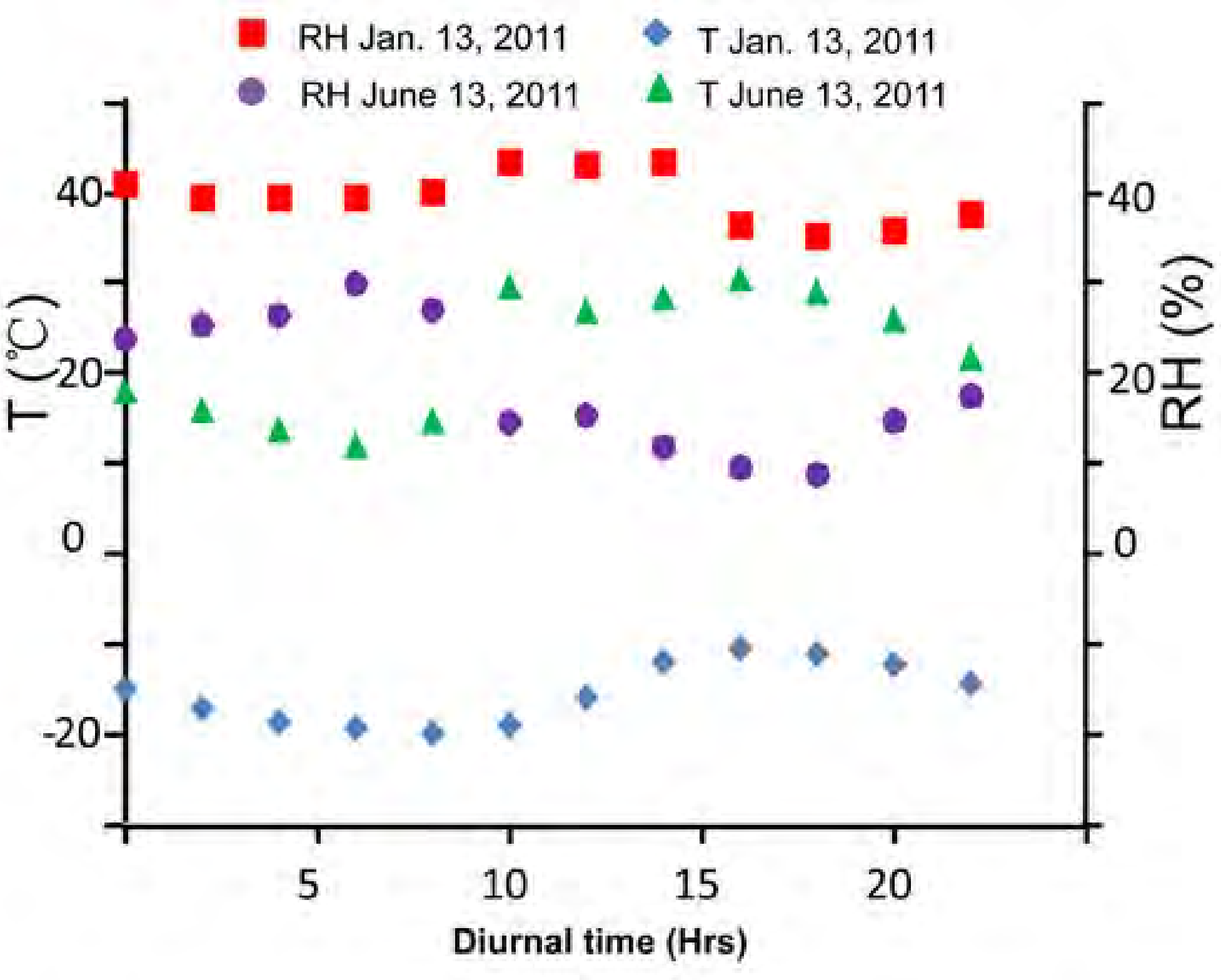
RH Jan. 13, 2011
T Jan. 13, 2011
RH June 13, 2011
T June 13, 2011
40
20
0
-20
T (°C)
RH (%)
5
10
15
20
Diurnal time (Hrs)

Minerals	Chemical formula
meridianiite	$MgSO_4 \cdot 11H_2O$
epsomite	$MgSO_4 \cdot 7H_2O$
hexahydrite	$MgSO_4 \cdot 6H_2O$, 6W
pentahydrite	$MgSO_4 \cdot 5H_2O$, 5W
starkeyite	$MgSO_4 \cdot 4H_2O$, 4W
sanderite	$MgSO_4 \cdot 2H_2O$, 2W
kieserite	$MgSO_4 \cdot 1H_2O$, 1W
halite	NaCl
carnallite	$KCl \cdot MgCl_2 \cdot 6H_2O$
gypsum	$CaSO_4 \cdot 2H_2O$
anhydrite	$CaSO_4$
mirabilite	$Na_2SO_4 \cdot 10H_2O$
glauberite	$Na_2Ca(SO_4)_2$

Vertical sections	Layers from the top surface to the bottom						
DP1	hexahydrite halite clays	halite	clays halite	halite clays	halite	clays halite	
DP2	clays carnallite halite	hexahydrite halite carnallite clays	clays halite hexahydrite	hexahydrite halite clays	halite hexahydrite clays	hexahydrite halite carnallite clays	clays halite
DP3	clays anhydrite	halite clays anhydrite glauberite	halite gypsum clays mirabilite	mirabilite halite gypsum			
DP4	clays anhydrite	halite clays anhydrite glauberite	halite gypsum clays mirabilite	mirabilite halite gypsum			